Preparation of a novel cartridge of SPE column using a new surface of heterocyclic azo ligand with modified activated carbon.

FAIQ F. KARAM , Ziyad T. Al-Khateeb

Department of Chemistry, College of Science, University of Al-Qadisiyah , Al-Diwaniya 58002, Iraq

Abstract

Disposable cartridges have been created using low-cost activated carbon produced from waste as solid support via using a chemical activation method, and modified with the new tridentate [N.N.O] donor azo ligand to yield a solid-phase sorbent, the thiazole azo 2-[2¯ -(5-nitro thiazolyl) azo]-4-methyl-5-nitro phenol (5-NTAMNP) derived from 2-amino-5-nitrothiazole and 3-methyl-4-nitrophenol by the diazotization operation and the adizonium chloride salt solution of 2-amino-5-nitrothiazole reacting with 3-methyl-4-nitrophenol as a coupling compound in alkaline alcoholic solution. The structure of ligand was identified and confirmed via resorting to various spectroscopic techniques which included, Proton nuclear magnetic resonance, Mass spectrum, UV–visible, Fourier-transform infrared (FTIR), X-Rays diffraction (XRD), the surface nature and morphology and size average and elemental composition of individual ligand particles were examined using a field emission scanning electron microscope (FE-SEM) coupled with an energy dispersive X-ray system (EDX), novel (5-NTAMNP)-modified activated carbon solid-phase sorbent were synthesized and characterized by chemical analysis by using, FT-IR, and XRD techniques and chelating sorbent were used as an adsorbent for the removal and for the determination of a hazardous heavy metallic ions Mn(II), Fe(III), Pb(II), Cu(II), in water under the optimum pH value for complexation with this azo ligand. The new (5-NTAMNP)-modified activated carbon showed highly effective solid phase extraction properties for these metallic ions.

Keyword: Activated carbon; NNO donor azo ligand; Solid-phase extraction; Disposable cartridges, SPE

1. Introduction

The concept of pollution refers to the situation in which a new material or input material is available or any effective effect in one of the environmental components, which limits its usefulness and is considered a disturbance that changes the characteristics of the natural environment, making it poor exploitation and benefit and not suitable in one way or another for life [1-2]. The pollution of heavy metals is considered an important category of pollution due to its perceived risks, which include causing significant damage to the environment and harming it greatly, and when its concentrations exceed the natural limits, which include changing environmental conditions such as pH, electrical conductivity (EC), oxidation reduction potential (ORP), and chemical oxygen demand (COD) change include the aquatic environmental in particular [3]. The increase use and recourse to of chemicals and metals in the various industrial processes is counterproductive, involving large quantities of liquid wastes containing high concentrations of toxic heavy metals. The presence of these gives environmental problems including how to eliminate, reduce their riskiness and find alternative means of disposal [4], it is therefore necessary to look for methods and

techniques to reduce this type of pollution as well as resort to reduce the impact of the toxicity and seriousness of pollutants before dumping or put them directly and the environment and it is necessary to do this in accordance with health conditions and an environment is effective predefined [5]. Effective removal of metal ions techniques requires the an exchange material so it can be easily recycling and enables it to functional in several environments via a great affinity for the metal of interest. Due to their physical and chemical properties [6], different instrumental analysis techniques have been employed to analyze the trace heavy metal ions in water, flame atomic absorption spectrometry (FAAS) is one of the technique have been used for heavy metal analysis, to enhance the detection sensitivity of the trace heavy metal ions in water, several pre-concentration methods have been developed. One of these methods solid phase extraction via using chelating sorbent [7-8]. SPE has been extensively used for the pre-concentration of metals in environmental waters [9], solid phase extraction (SPE) is pre-concentration technique and favorably proposed to preconcentrate trace elements from matrices that adversely influence atomic absorption spectrometric detection [10], and it is the most frequently technique as the separation and preconcentration of trace metals, and for the determination of element in aqueous samples and employed to increase the sensitivity of (FAAS) owing to the high effective, fast, and simple pretreatment procedure to achieve pollutant/matrix separation and preconcentration [11-13]. SPE sorbents used for metal determination can be chemically modified with the presences of complexing agents, trace metals can also be complexed with ligands loaded in several supports such as activated carbon (AC) was the sorbents utilized in their unmodified forms in a number of applications most applications involve selective retention of the analyte on a solid phase extraction column and the fine distribution of chemicals and/or metal particles in the pores of AC it is known by term the impregnation [14-17]. Thiazolylazo agents have been successfully employed in determinations of many metal ions and have attracted much attention as they are sensitive chromogenic reagents for spectrophotometric, liquid chromatography and extraction- photometric such as solid phase, liquid–liquid and cloud point extraction owing to the high sensitivity and selectivity therefore these azo reagents have attracted much attention in analytical field [18]. The main objective of this work, prepared a low-cost activated carbon from wastes of (olive kernel , pistachio shells) by chemical activation and modified with synthesis of novel thiazolyl azo ligand, azo dye ligand (5-NTAMNP) synthesis to yield novel a solid-phase sorbent and was to test the ability of activated carbon, (5-NTAMNP)-modified activated carbon to remove heavy metals from water. Due to the presence of oxygen, sulfur and nitrogen atoms in its structure. The proposed method used as a solid-phase extractor for determination and removal of Mn(II), Pb(II), Fe(III) and Cu(II) high concentrations in water samples.

2. Experimental

2.1. Materials & Methods

All solvents, organic chemicals and inorganic salts those used in the present work, were all highly purified and directly used without any further purification, chemicals supplied from Sigma-Aldrich, Merck, BDH, Fluka, Scharlau, Companies, Stock solutions were prepared by dissolving a required amount of chloride salt of each Fe, Mn and Cu , and Pb solutions were prepared by dissolving a required amount of acetate salt

in ammonium acetate buffer solutions, and then dilution of the stock solution in double distilled water with a concentration of 1000 mg L^{-1} for all metallic ions, and these solutions were diluted daily to obtain working solutions, 2-[2-(5-nitro thiazolyl) azo]-4-methyl-5-nitro phenol (5-NTAMNP) solution (0.03% (m/v%)) was prepared by dissolving a certain weight of the organic reagent in the absolute ethanol, and PVA solution (0.1% (m/v%)) was prepared in hot distal water.

2.2. instrumentation

The ^{1}H-NMR spectra were carried out on a Bruker model 500-UltraShield 300 MHZ spectrometer using DMSO-d_6 as solvent for measurement and using TMS as an internal standard reference. Mass spectra were collected on a Shimadzu Agilent Technologies model 5973C. Fourier Transform Infrared (FT-IR) spectra were recorded on a Shimadzu model 8400s FT-IR spectrometer scanning at range between (4000-400cm^{-1}) via a KBr disk. UV-Visible spectra were measured on a Shimadzu model UV-1650 UV-Visible spectrophotometer Double beam scanning at range of (200-1100nm) using absolute ethanol as solvent for measurement. X-ray diffraction were performed on Shimadzu model XRD-6000 spectroscopy. The field emission scanning electron microscope and the energy dispersive X-ray were taken on a TESCAN model MIRA3 (FE-SEM). The detection of metal ions was performed using a Shimadzu, Japan, atomic absorption spectrometer technique, type AA-7000F, equipped with a hollow cathode lamp as radiation source and a deuterium background corrector at the respective wavelengths using an air-acetylene flame according to the instrumental parameters recommended by the manufacturer. The set instrument parameters were those recommended by the manufacturer (Table1). And also used JENWAY, England model 3505 digital pH meter for the pH adjustment. The Melting points were taken in open capillary tube by using OMEGA Digital Melting Point Apparatus model MPS10-120.

2.3. Synthesis of azo dye ligand
2-[2- -(5-nitro thiazolyl) azo]-4-methyl-5-nitro phenol (5-NTAMNP)

Synthesized of the novel azo ligand according to the method proposed by Al-Adilee et al. [19-20], with some modification via the diazotization coupling reaction (Scheme 1). This method of action included dissolving (1.45g, 0.01mol) from 2-amino-5-nitrothiazole in mixture contain (5ml of concentrated HCL) and (35ml of distilled water) then the all mixture was cooled to (0-2)℃, then to this solution was added drop wise a solution of sodium nitrite prepared by dissolving (0.9g, 0.013mol of $NaNO_2$) in 30ml of distilled water, and stirred for (30min) at (0-5)℃. The resulting diazonium chloride solution was added also drop wise while maintaining temperature at (0-5)℃ , with stirring continuously into a 500 mL beaker containing (1.53g, 0.01mol of 3-methyl-4-nitrophenol in the mix contains on 50ml of absolute ethanol & 18ml of 10% NaOH) and coolant to (0-5)℃ , after completion of the add-on process the final mixture was stirring at least for (2h) then complete the precipitate of the ligand by modifying the acidic function of the solution to pH =6.5.and allowed to stand overnight.

The precipitate was filtered off , washed with distilled water and finally recrystallized. The ligand is spectrally studied and check of purity via TLC techniques. The melting point of azo ligand point found to be (129-131℃) and the yield was of about 82%. The ligand appearance was as a reddish brown rod crystals. The following chart illustrates the method of preparation azo dye (5-NTAMNP) :

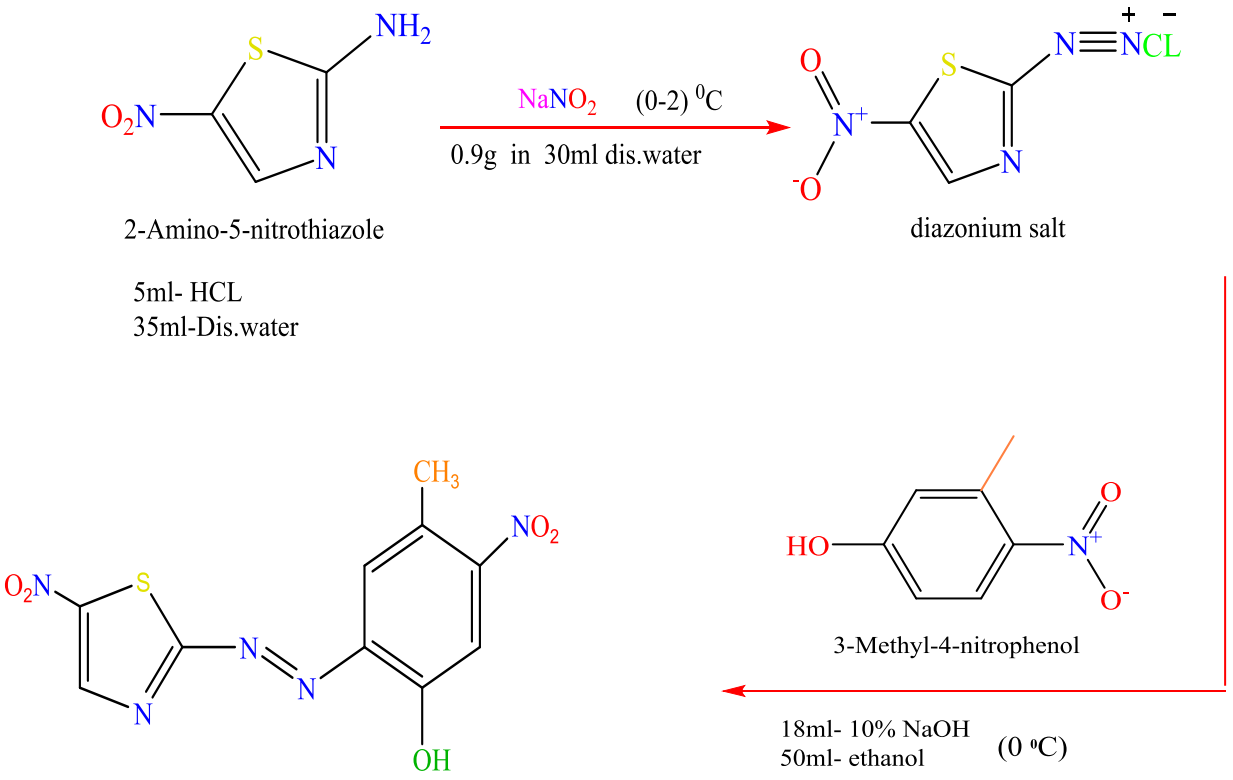

2-[2-(5-Nitrothiazolyl)azo]-4-methyl-5-nitrophenol

(5-NTAMNP) $pH = 6.5$

Scheme 1. Synthesis of thiazolyl azo dye ligand (5-NTAMNP).

2.4. Preparation of activated carbon

Agricultural wastes resulting from human activities, which including raw materials (olive kernel, pistachio shells) was Collect and used for the preparation of activated carbons by using chemical activation method. The collected agricultural wastes were washed them well with hot distilled water to remove dust and to get rid of impurities and of the fibers, and then completely dried in sun light for days and the material was finally sieved to discrete sizes. After thoroughly confirming the dryness (olive kernel, pistachio shells), taking the raw materials weights before the carbonization process. The raw materials was then

carbonized at 675 ℃ under nitrogen atmosphere for 1 h (first pyrolysis). A certain amount of produced char powder then was soaked with 25% solution of calcium chloride ($CaCL_2$). The final mixture was form is a homogeneous dough and left for 24 hours. and activated in a muffle furnace kept (second pyrolysis) at 800 ℃ for a period of 10 min. A chemical activation process is performed to increase the surface area of the coal. The activated product (OK-AC), (PS-AC) was then cooled to room temperature and washed with deionized water to remove remaining chemical Wash activated charcoal with distilled water and dry under 250 ℃ for half an hour after the drying phase, activated carbon is ready for use.

2.5. Characterization studies

Moisture content (%) by mass, Ash content (%) by mass, Bulk density, Particle Density, Porosity, pH, Pore volume, Volatile materials (%), Charring yield (%) , Fixed carbon (%) were analyzed as per standard procedures [21-23] for (OK-AC), (PS-AC) and the important physic-chemical/structural parameters values used in this work were listed in Table 2.

2.6. Preparation of 2-[2¯ -(5-nitro thiazolyl) azo]-4-methyl-5-nitro phenol (5-NTAMNP)-modified activated carbon

The modification of the activated carbon was performed as described in the according to method reported in the literature [24-26], with some modification. Activated carbon (0.5 g) was added into 25 mL of 0.03% (m/v) 2-[2¯-(5-nitro thiazolyl) azo]-4-methyl-5-nitro phenol (5-NTAMNP) solution, and the Prepare a 0.03% solution of NTAMNP and the process of preparing the solution (NTAMNP) daily, and the mixture with continuous stirring for 12 h. Then, the 2-[2¯-(5-nitro thiazolyl) azo]-4-methyl-5-nitro phenol (5-NTAMNP)-modified activated carbon was filtered off, and washed with appropriate amount of deionized water until filtrate was dried at 100 ℃. (5-NTAMNP)-modified activated carbon was obtained. Synthesized (5-NTAMNP)-modified activated carbon was characterized by XRD and FT-IR spectroscopy.

2.7. Test procedure for preconcentration & removal

4.0 mL of buffer solution were added to 6.0 mL of solution containing $1\text{-}5\times10^{-4}$ M of the each working element to achieve the desired pH between 6.0 and 7.5. Before lode the (5-NTAMNP)-modified activated carbon a some amount of a binder of 0.1% (m/v) Poly vinyl alcohol solution was coated the inner part of cartridges that holds materials (5-NTAMNP)-modified activated together to bottom of the cartridges and to prevent the loss of a solid-phase sorbent when the sample solution passed through the cartridges, then (5-NTAMNP)-modified

activated carbon (0.5 g) was packed into a cartridges (15 mm i.d., 8.89 cm long) and preconditioned with 10 ml of the buffer solution (pH-6.0). The polypropylene cartridges was preconditioned with the buffer solution. Buffered metal test solution was then passed through the column at 3 mL min^{-1} under gravity. After applying the sample solution. The residual heavy metals were determined by flame atomic absorption spectrophotometer (FAAS) analysis.

Table 1: OPERATING PARAMETERES OF ATOMIC ABSORPTION ANALYSIS.

Metal	Wavelength (HCL)(nm)	Slit width (nm)	HCL current (mA)	Flame composition
Cu	324.8	0.5	6	Air-Acetylene
Fe	248.3	0.2	12	Air-Acetylene
Pb	283.3	0.5	10	Air-Acetylene
Mn	279.5	0.2	10	Air-Acetylene

HCL: Hallow Cathode Lamp

3. Results and discussion

3.1. Physical & chemical properties of azo dye ligand (5-NTAMNP)

The azo dye ligand (5-NTAMNP) is characterized by the fact that his amorphous look is on the form of a fine brownish-red powder, while its crystalline appearance is show as like a micro needle/rod-shaped crystals, giving the color red-purple when dissolved with ethanol. This synthesis thiazolylazo ligand is easily soluble in most solvents [Acetone, THF, DMSO, DMF, Methanol, Ethanol] but it is sparingly soluble in water. The purity of the ligand was confirmed by thin layer chromatography (TLC) technique via using certainly solvent system methanol: water: acetic acid (12:3:7v/v) [27], this ligand conferred a single red purple color spot when its adsorbed onto silica chromatography plates.

3.2. ^{1}H NMR spectra

The ^{1}H NMR spectra for novel ligand (5-NTAMNP) [28-29] was obtained in DMSO-d_6 as solvent with TMS as an internal reference (300MHZ). The spectrograph which is illustrated in Figure.1. is interpreted as follows: a Singlet at δ=2.510-2.505 ppm corresponding to the three protons in CH_3 group at C3 on phenolic ring, a Single between 6.788-6.772 ppm corresponding to the aromatic protons at C3, and C6 of the phenolic ring, a Singlet at δ=8.006-7.966 ppm corresponding the H4 proton of the thiazole ring, a Singlet at δ=10.789 ppm corresponding to the OH proton of the phenol ring.

3.3. Mass spectra

The mass spectral of free novelty ligand (5-NTAMNP) are presented in Figure.2, the mass spectra show the base peak M^+ at M/Z^+= (309.26) correspond to the original molecular weight of ligand molecular ion, the molecular ion of the reagent with reactive abundance equal to (1.4%), where the mass spectrum was given to ligand a number of fragmentation and these fragmentation represented in the mass spectra in term of relative abundance compared to M/Z^+, and the main peak show via mass spectrum is relatively to molecular weight of ligand $[C_{10}H_7N_5O_5S]^+$, the schem.2. explains the proposed mass fragmentation products for ligand (5-NTAMNP) [30-31].

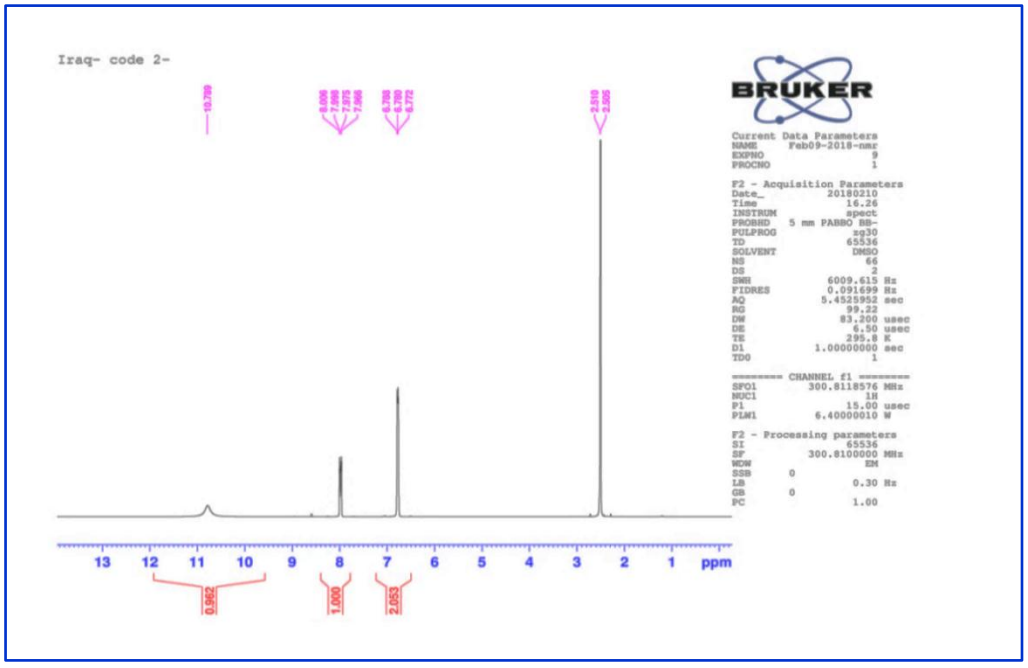

Figure. 1. ^{1}H NMR spectrum of thiazolylazo dye ligand (5-NTAMNP).

3.4. Electronic spectra measurements

The electronic absorption spectra of thiazolylazo dye ligand (5-NTAMNP) were measure at (10^{-3} M) via used absolute ethanol as solvent to them, the ligand many of specific absorbance bands at differ wavelength due to the electronic transitions for them [32-33]. These bands are appearing at the position 236 nm(42373 cm^{-1}), 408 nm (24510 cm^{-1}) and 519 nm (19268 cm^{-1}). The first band can be attributed to a n-σ*, transmission of hydroxyl group (OH) in the aromatic ring. And the second band can be attributed to transition π-π* of the two interacting (C=C) group of aromatic and thiazole rings. While the third band is due to the n-π* transition resulted from the presence of group containing double bond, in addition to the presence of hetero atom carrying a ion pair of electrons in thiazole ring in addition to intermolecular charge transfer taken place from phenyl

ring to the thiazole ring through the azo group (-N=N-). The UV-visible spectra of azo ligand (5-NTAMNP) are shown in Figur.3.

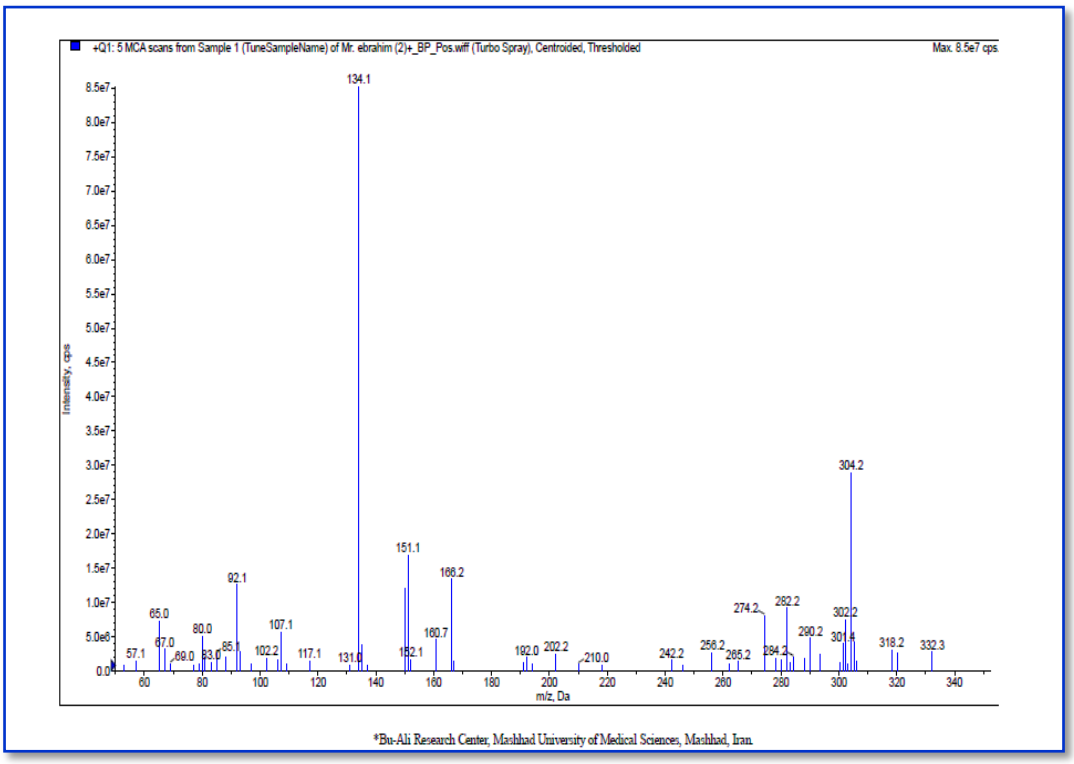

Figure. 2. Mass spectrum of thiazolylazo dye ligand (5-NTAMNP).

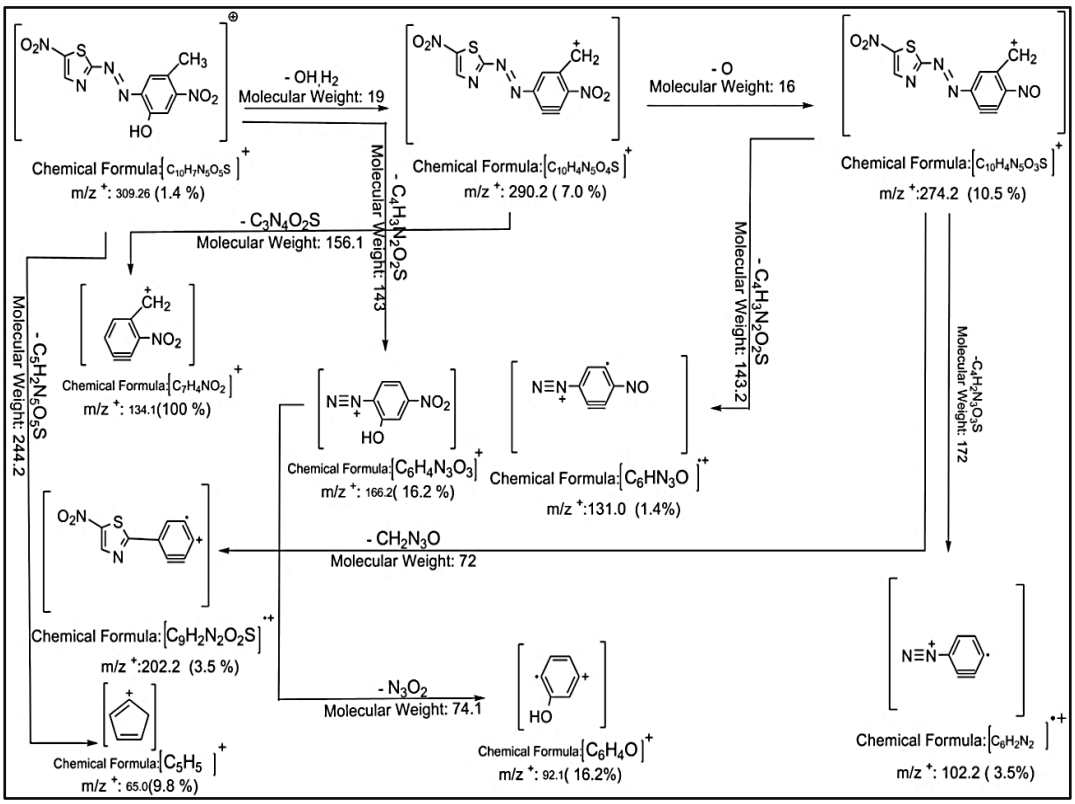

Scheme 2. Mass spectrum fragmentation of thiazolylazo dye ligand (5-NTAMNP).

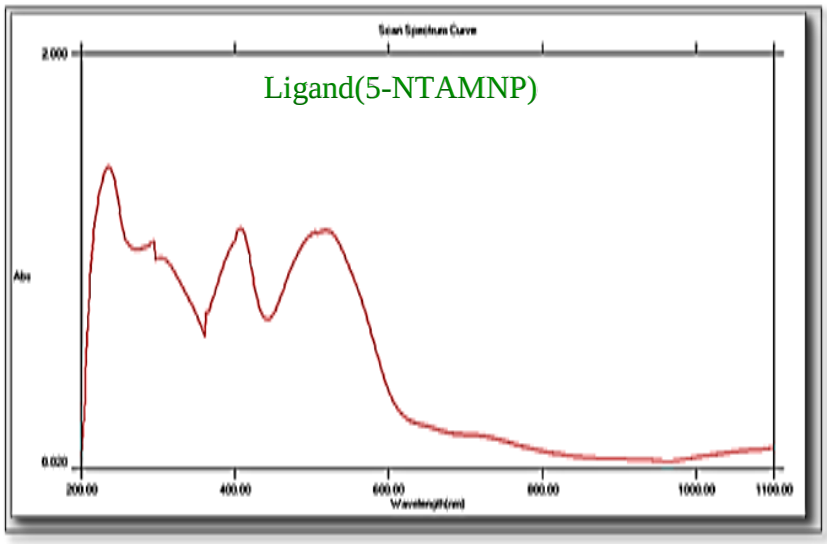

Figure. 3. UV-visible spectra of ligand (5-NTAMNP).

3.5. Infrared spectra measurements

The infrared spectra of ligand (5-NTAMNP), prepared (OK-AC), (PS-AC) active carbon and solid-phase sorbent (5-NTAMNP)-modified activated carbon are shown in Figure 4, 5 and 6. The spectrum of azo ligand (5-NTAMNP) shows a broad and strong absorption band around 3309.62 cm^{-1} due to γ (O-H) group in the azo dye ligand. The IR spectrum of the ligand showed a week band had been observed at 2985.60 cm^{-1} which may be attributed to the aliphatic γ (C-C-H) assignable to the methyl group of imidazole ring, while the band at 3093.61cm^{-1} represented to the stretching vibration of aromatic γ (C=C-H), and the whilst the spectrum of ligand show another bands at 1589.23 cm^{-1} and 1419.51 cm^{-1}
Which they are corresponding to the γ (C=N) and γ (C=C) groups, respectively. Due to thiazole and phenolic ring vibrations. Two strong absorption bands are observed at 1512.09 cm^{-1} and 1319.22 cm^{-1} in the 5-NTAMNP spectrum, attributable to stretching vibrations γ (-NO_2) group in the azo dye ligand. A medium intensity band at 1473.51 cm^{-1} in the azo dye ligand was attributed to γ (N=N) stretch of the azo group and the strong band at 1257.5 cm^{-1} also appears in the ligand spectrum and this absorption band is due to γ (C-S) of thiazole ring [34-36]. The infrared spectra of (olive kernel, pistachio shells) activated carbons are illustrated in Fig. 5(a, b). The samples spectra showed a medium absorption band around 1700 cm^{-1} refers to the stretching vibrations of γ (C=O)bonds Also, the peak detect at 1425 cm^{-1} has been assigned to stretching vibrations of γ (C-C) bonds. The peak around (1600 cm^{-1}) shows the presence of stretching vibration of bonds γ (C=O) in carbonyl groups and It refers to stretching vibrations in the aromatic ring coupled to that of highly conjugated carbonyl groups (C=O), while the bands between 1100-1200 cm^{-1} refers to stretching vibrations of γ (C-C) bonds and Similarly, Weak broad absorption bands around 3741 cm^{-1} may also

represent γ (O-H) group stretching vibration in phenol or alcohol on the surface. A weak absorption bands are observed 3247-3286 cm^{-1} in the (OK-AC), (PS-AC) active carbon spectrum, attributable to stretching vibrations of γ (H-C≡C) in unsaturation; alkyne groups, a peak located at 2360.71 cm^{-1} and this peak indicated the presence of γ (C≡C) stretching vibrations in alkyne groups. And these peak around 3000-2800 cm^{-1} is γ (C-H) stretching vibration in methyl and methylene group. Finally in the spectra of all active carbon samples there are bands in the region of 860–600 cm^{-1} indicate aromatic γ (C-H) bending [37-39]. The Figure.6. shown infrared spectra of solid-phase sorbent (5-NTAMNP)-modified activated carbon, where the spectrum showed an absorption band at wavenumber around 3502.49 cm^{-1} is assigned to stretching vibration of γ (O-H) bonds. Furthermore, It exhibition new band in the region of 1473.51 cm^{-1} owing to the presence of γ (N=N) stretching vibrations, this band appeared at the same region that azo group (N=N) had already appeared in the infrared spectra of ligand (5-NTAMNP). While the γ (C=N) and γ (C=C) stretching vibrations have been shifted to frequencies, 1542.95 cm^{-1}, 1396.37 cm^{-1}, respectively Due to the linkage between the groups of active carbon surfaces and the azo ligand after the chemical modification process occurred. Thus, we can say that (OH), (N=N) and (C=N) groups formed important position for coordinates in this new type of solid-phase sorbent (5-NTAMNP)-modified activated carbon.

Table 2. PHYSICO-CHEMICAL PROPERTIES OF (olive kernel, pistachio shells) ACTIVATED CARBON

NO.	PROPERTIES	PS-AC	OK-AC
1	***Moisture content, %***	4.23	2.29
2	***Volatile materials, %***	47.75	39.38
3	***Ash content, %***	2.70	6.83
4	***pH***	7.87	8.33
5	***Pore volume, ml/g***	1.01	0.56
6	***Porosity, %***	0.52	0.67
7	***Bulk density, g ml^{-1}***	0.478	0.591
8	***Charring yield, %***	15.34	25.84
9	***Fixed carbon, %***	45.32	51.5
10	***Particle Density ml/g^{-1}***	0.99	1.79

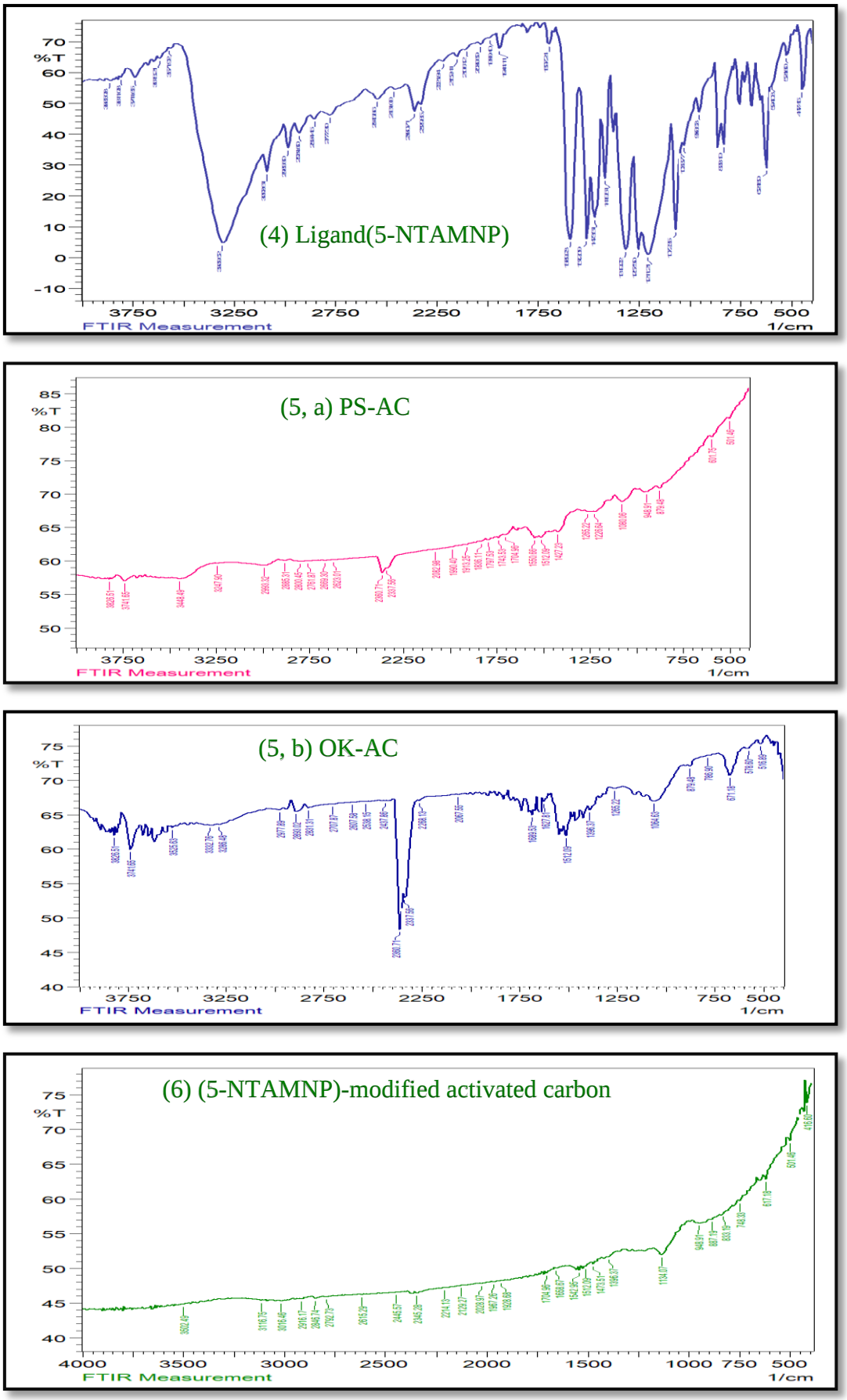

Figure (4, 5 and 6) FTIR analysis of ligand, active carbon and ligand-modified active carbon.

3.6. X-ray diffraction study (XRD)

The (XRD) of ligand (5-NTAMNP) were recorded in the range of 2Θ = (10-80 deg) value in its solid state using the (Cu-kα) copper spectrum band as a generator of the X-ray with wavelength λ =1.54056Å, X-ray diffraction spectroscopy was used to identify the crystalline structure and to determine the (grain size) crystal size , d-spacing between the atomic levels of the ligand . The Figure(7) of (XRD) spectra shows that the ligand appeared as a (Poly-crystalline) system and these systems are of different sizes and random distribution in nature [40], the XRD spectra of pure ligand display three main sharp peak at [2θ =27.1249, 13.6297, 13.9383] that corresponded to d-spacing of [d= 3.28479, 6.49158, 6.34854 Å], these major peaks represented the preferred orientation of crystal growth of the ligand molecule. The appearance of high intensity peak indicates a high crystalline nature. To calculate d-spacing reflections were obtained using Bragg's equation n λ = 2dsinΘ, where d is the spacing between the crystalline levels, n is an integer (1,2,3 …), λ is the wavelength of X-ray Cu-kα = 1.54056 Å, Θ is the diffraction angle [41]. The grain size of the particles were evaluated by the Debye–Scherrer [42]. D = k λ /βCos Θ, where D is the average grain size, k is Blank's constant (0.94), λ is the X-ray wavelength (0.154059 nm), and Θ and β are the diffraction angle and full width at half maximum of an observed peak, respectively. Figure (8) shows the XRD profiles of the prepared (OK-AC), (PS-AC) active carbon. The activated carbon samples with broad peaks that revealed predominantly amorphous structure, which is an advantageous property for well-defined porous adsorbents. The broad diffraction peaks found at around 24^{o} confirm that the active carbon samples formation of the turbostratic structure of disordered carbon and can have high micro-porous structure while. The other sharp peaks observed confirmed the presence high degree of crystallinity of this sample and related to the graphitic plane and it confirms that the activated carbon samples are more graphitic in nature and indicates that the carbon can be regarded as a partly graphitized carbon. The XRD spectra of prepared (OK-AC), (PS-AC) active carbon display two main sharp peak at [2θ =23.1548, 29.3932] that corresponded to d-spacing of [d= 3.83823, 3.03626 Å], and these major peaks represented the preferred orientation of crystal growth of the activated carbon [43-45]. Figure (9) the XRD spectra of solid-phase sorbent (5-NTAMNP)-modified activated carbon display a three peaks at at [2θ =24.9312, 23.0151, 29.3481] that corresponded to d-spacing of [d= 3.56863, 3.86121 , 3.04082 Å]. While the process of impregnation with these azo dyes led to increased growth or crystalline nature of the prepared a solid-phase sorbent. Table.3. shows the diffraction angles, d-spacing values, and the crystalline size of prepared ligand, (OK-AC), (PS-AC active carbon and solid-phase sorbent (5-NTAMNP)-modified activated carbon.

Table 3: 2Θ VALUE OF EACH PEAK, RELATIVE INTENSITY, d-spacing FWHM, LATTICE STRAIN and CRYSTALLITE SIZE.

Compounds	2Θ	FWHM	I/I_1%	Lattice Strain	D(nm)	d-spacing
Ligand(5-NTAMNP)	13.6297	0.23970	100	0.0088	34.88	6.49158
	27.1249	0.25970	84	0.0047	32.88	3.28479
	13.9383	0.19860	45	0.0071	42.11	6.34854
Active carbon	29.3932	0.31170	100	0.0052	27.53	3.03626
	23.1548	0.66660	45	0.0142	12.7099	3.83823
(5-NTAMNP)-modified activated carbon	29.3481	0.26560	100	0.0044	32.31	6.49158
	23.0151	0.54660	29	0.0117	15.5	3.28479
	24.9312	0.40000	28	0.0079	21.25	6.34854

3.7. EDX & FE-SEM analysis

The morphology and the Topography for ligand (5-NTAMNP) is identified using FE-SEM, the Figure.10(a, b). Show FE-SEM and EDX spectra analysis of ligand. FE- SEM image shows the ligand (5-NTAMNP) where the nature of homogeneity of the surface and the distribution of particles and collected in an irregular order, and illustrated the surface shape of the ligand on it as horizontal Micro-slices with granular appearance and has average size up to 96.91nm, these slices had different diameters and contain cavities containing pores and possess a high degree of ruggedness.

The EDX image shows that the prepared ligand includes only sulfur, carbon, nitrogen, and oxygen is similar to the chemical composition for azo ligand. This indicates a match in the atomic structure and to the purity of the synthesis azo ligand (5-NTAMNP). The EDX spectrum referred to weight percentage of each element within the composition of the ligand.

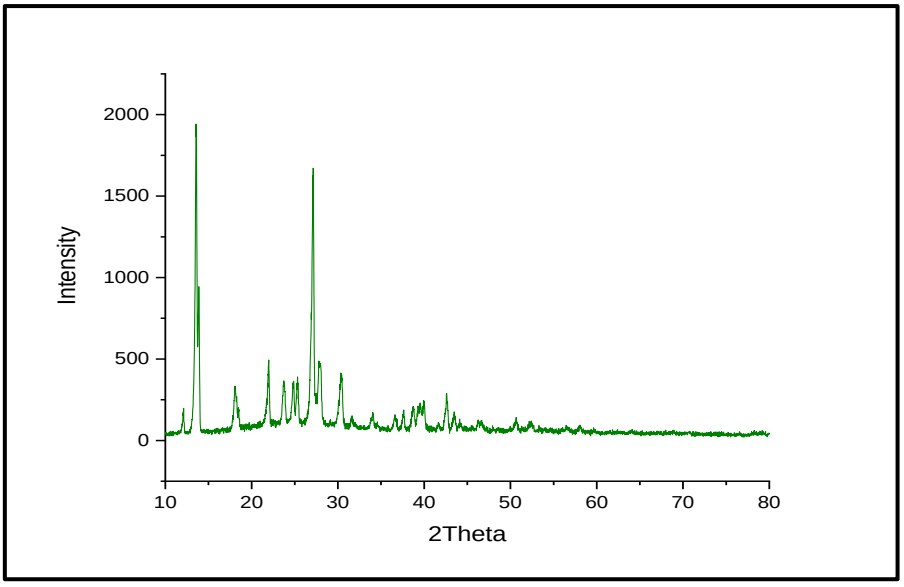

Fig. 7. XRD spectra of ligand(5-NTAMNP).

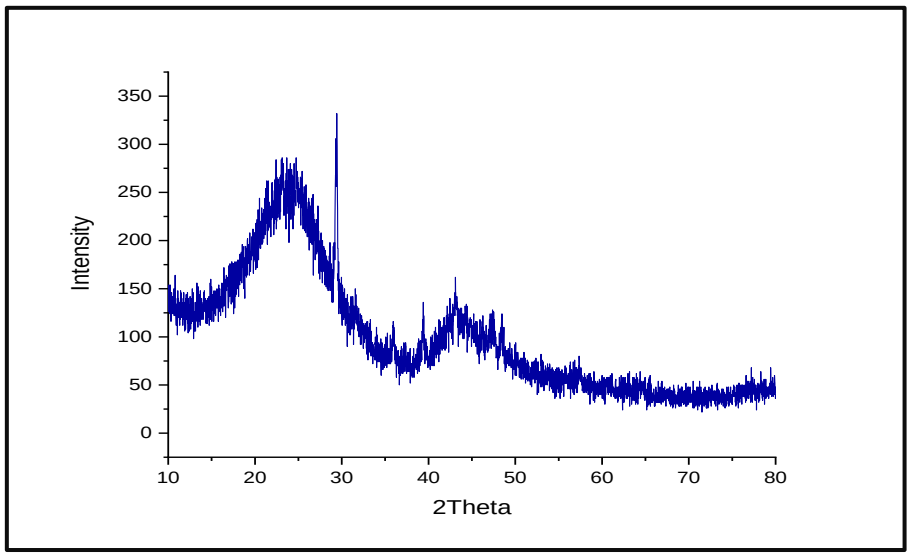

Fig. 8. XRD spectra of ligand(5-NTAMNP).

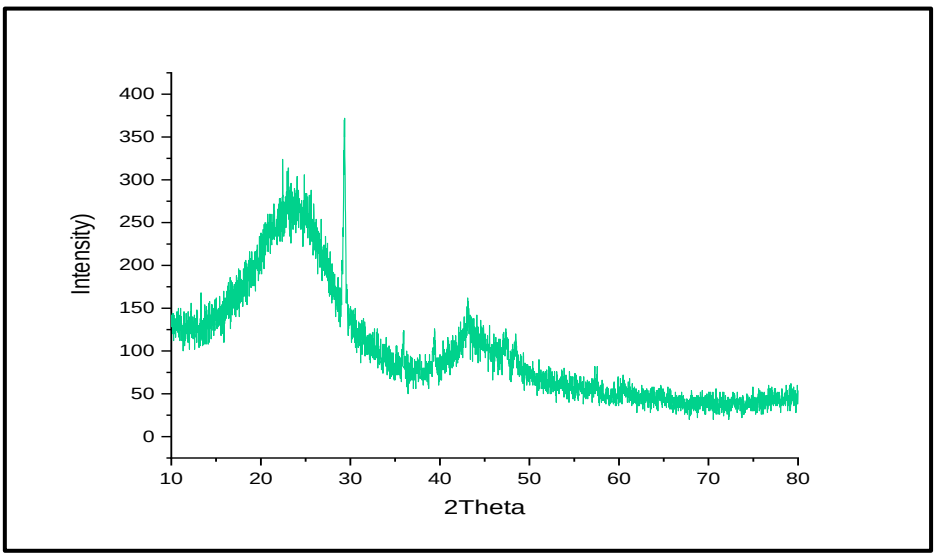

Fig. 9. XRD spectra of ligand(5-NTAMNP).

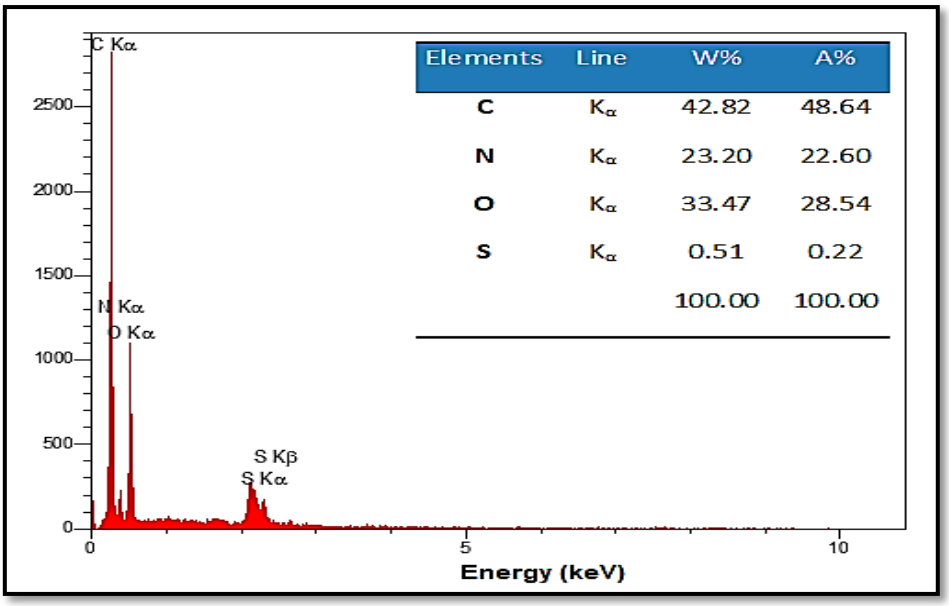

Fig. 10. (a) EDX spectra of ligand(5-NTAMNP).

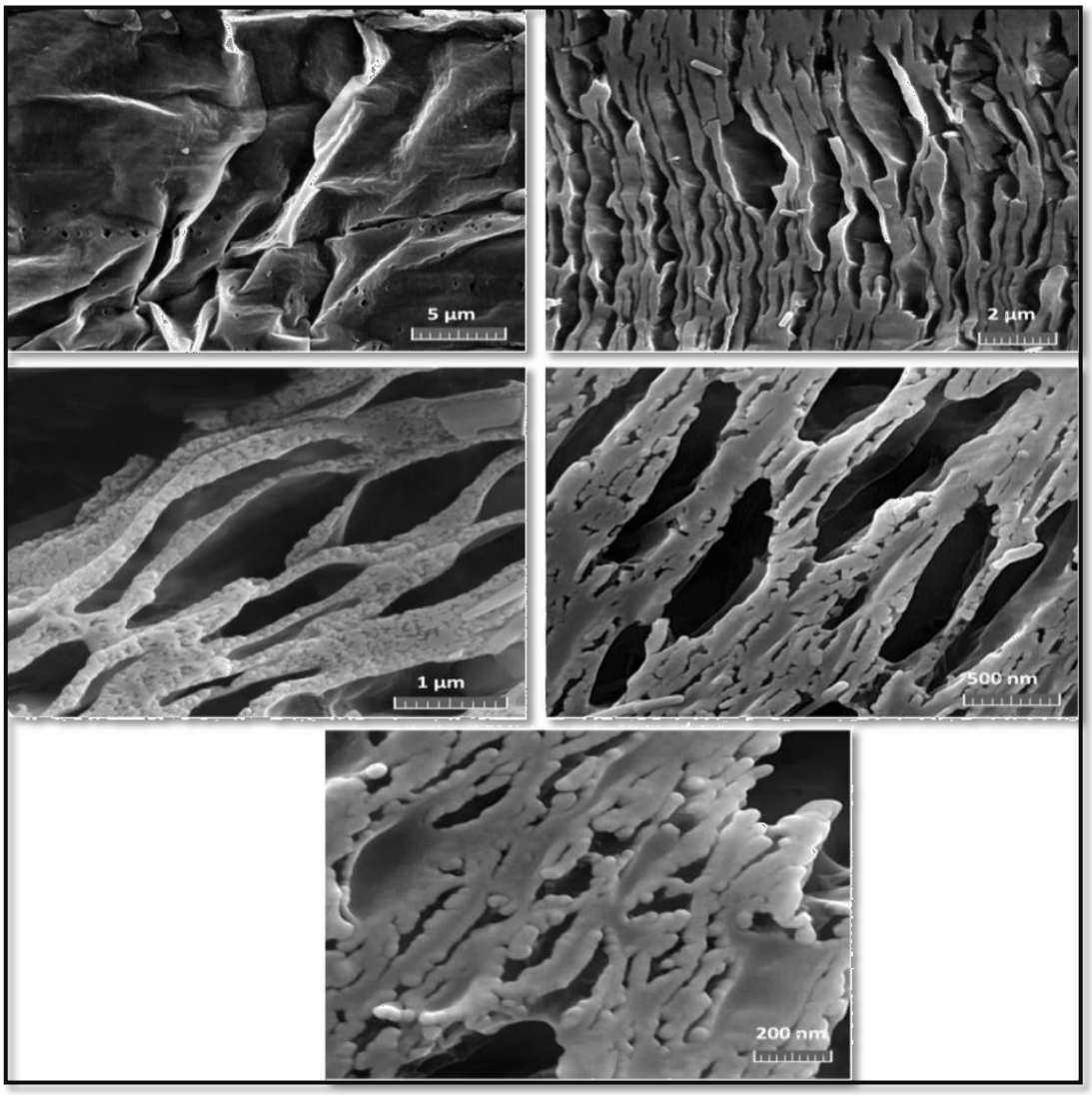

Fig. 10. (b) FE-SEM images of ligand (5-NTAMNP)

3.8. Evaluation of the method

The precision and the sensitivity of the method was evaluated under the optimized conditions of the investigated elements, as R.S.D., limit of detection (LOD) and the limit of quantification (LOQ) of the procedure for the determination of analytes. Removal efficiency were found to be 99.8%, 89.73% , 90.60% and 99.14% for Fe(III), Pb(II), Mn(II), and Cu(II) ions, respectively. The relative standard deviations (RSDs) for three replicates were found to be 1.4%, 0.197%, 0.166% and 2.03% for Fe(III), Pb(II), Mn(II), and Cu(II) respectively. The LOD for Fe(III), Pb(II), Mn(II), and Cu(II) was 0.042 ppm, 0.75 ppm , 0.239ppm and 0.027ppm respectively. The results are summarized in Table 4.

Table 4. Analytical characteristics of the presented procedure

Parameters	Fe(III) (81.105 ppm)	Pb(II) (32.529 ppm)	Mn(II) (98.995 ppm)	Cu(II) (17.048 ppm)
RSD%	1.4	0.197	0.166	2.03
LOD	0.042	0.75	0.239	0.027
LOQ	0.140	2.5	0.79	0.09
S.D	0.002	0.006	0.0155	0.002
$\overline{X}$	0.162	3.34	9.305	0.146
Slope	0.1426	0.024	0.1943	0.2233
R%	99.8	89.73	90.60	99.14

R%: The percentage of removal efficiency

4. Conclusions

Based on this experimental study, the following conclusions were reached: we have prepared and structurally characterized of new azo chelating ligand (5-NTAMNP) derived from thiazole. The structure of analytical reagent has been confirmed by the analytical data (EDX), mass spectrum, 1H NMR, FT-IR and electronic spectra. The azo ligand have different morphologies as appeared in XRD and SEM. The use of (5-NTAMNP)-modified activated carbon as solid phase extraction sorbent For (FAAS) determination of Mn(II), Fe(III), Pb(II) and Cu(II) has been established in the present work for the analysis of heavy metals in aqueous solution and for preconcentration of the heavy metals prior to their determination by (FAAS) analysis, proved to be a simple, fast and economic solid phase extraction procedure technique. The a new solid-sorbent showed a greatest

affinity towards metallic ions with highest successfully removal percentage. The proposed SPE method was more efficient for the preconcentration of Fe(III), and Cu(II) than other methods described in the literature, the comparative data from recent papers on (5-NTAMNP)-modified activated carbon and other solid phase extraction studies were given in Table 5.

Table 5. Comparison of the proposed SPE procedure with other methods described in the literature.

Adsorbent used for SPE	LOD (µg L^{-1})	Reference
Multiwalled carbon nanotubes with a D2EHPA-TOPO mixture	Cu: 50	46
Amberlite XAD-4/di-2-pyridyl ketone Thiosemicarbazone	Cu:30 , Fe: 50	47
Phenylpiperazine dithiocarbamate Complexes on activated Carbon	Cu: 15 , Pb: 56 , Mn: 17	48
(5-NTAMNP)-modified activated carbon	Cu: 27 , Pb: 750 Fe: 42 , Mn: 239	This work

References

1. Hill, M. K. (2010). *Understanding environmental pollution*. Cambridge University Press.
2. Khan, M., & Ghouri, A. M. (2011). Environmental pollution: its effects on life and its remedies.
3. Zhang, Z., Juying, L., Mamat, Z., & QingFu, Y. (2016). Sources identification and pollution evaluation of heavy metals in the surface sediments of Bortala River, Northwest China. *Ecotoxicology and Environmental Safety*, *126*,94-101.
4. Ahluwalia, S. S., & Goyal, D. (2007). Microbial and plant derived biomass for removal of heavy metals from wastewater. *Bioresource technology*, *98*(12), 2243-2257.
5. Abdolali, A., Ngo, H. H., Guo, W., Zhou, J. L., Zhang, J., Liang, S., ... & Liu, Y. (2017). Application of a breakthrough biosorbent for removing heavy metals from synthetic and real wastewaters in a lab-scale continuous fixed-bed column. *Bioresource technology*, *229*,78-87.

6. Popa, C., Bulai, P., & Macoveanu, M. (2010). THE STUDY OF IRON (II) REMOVAL FROM 34% CALCIUM CHLORIDE SOLUTIONS BY CHELATING RESIN PUROLITE S930. *Environmental Engineering & Management Journal (EEMJ)*, *9*(5).

7. ALOthman, Z. A., Habila, M., Yilmaz, E., & Soylak, M. (2012). Solid phase extraction of Cd (II), Pb (II), Zn (II) and Ni (II) from food samples using multiwalled carbon nanotubes impregnated with 4-(2-thiazolylazo) resorcinol. *Microchimica Acta*, *177*(3-4), 397-403.

8. Zhao, F., Chen, Z., Zhang, F., Li, R., & Zhou, J. (2010). Ultra-sensitive detection of heavy metal ions in tap water by laser-induced breakdown spectroscopy with the assistance of electrical-deposition. *Analytical Methods*, *2*(4), 408-414.

9. Kocot, K., Zawisza, B., Marguí, E., Queralt, I., Hidalgo, M., & Sitko, R. (2013). Dispersive micro solid-phase extraction using multiwalled carbon nanotubes combined with portable total-reflection X-ray fluorescence spectrometry for the determination of trace amounts of Pb and Cd in water samples. *Journal of Analytical Atomic Spectrometry*, *28*(5), 736-742.

10. El-Shahawi, M. S., Bashammakh, A. S., Orief, M. I., Alsibaai, A. A., & Al-Harbi, E. A. (2014). Separation and determination of cadmium in water by foam column prior to inductively coupled plasma optical emission spectrometry. *Journal of Industrial and Engineering Chemistry*, *20*(1), 308-314.

11. BItirmis, B., Trak, D., Arslan, Y., & KENDÜZLER, E. (2016). A Novel Method Using Solid-Phase Extraction with Slotted Quartz Tube Atomic Absorption Spectrometry for the Determination of Manganese in Walnut Samples. *Analytical Sciences*, *32*(6), 667-671.

12. Türker, A. R. (2007). New sorbents for solid-phase extraction for metal enrichment. *Clean–Soil, air, water*, *35*(6), 548-557.

13. Habila, M., Yilmaz, E., ALOthman, Z. A., & Soylak, M. (2014). Flame atomic absorption spectrometric determination of Cd, Pb, and Cu in food samples after pre-concentration using 4-(2-thiazolylazo) resorcinol-modified activated carbon. *Journal of Industrial and Engineering Chemistry*, *20*(6), 3989-3993.

14. Jankowski, K., Jackowska, A., & Łukasiak, P. (2005). Determination of precious metals in geological samples by continuous powder introduction microwave induced plasma atomic emission spectrometry after preconcentration on activated carbon. *Analytica chimica acta*, *540*(1), 197-205.

15. Soliman, E. M., Saleh, M. B., & Ahmed, S. A. (2004). New solid phase extractors for selective separation and preconcentration of mercury (II) based on silica gel immobilized aliphatic amines 2-

thiophenecarboxaldehyde Schiff's bases. *Analytica Chimica Acta*, *523*(1), 133-140.

16. Daorattanachai, P., Unob, F., & Imyim, A. (2005). Multi-element preconcentration of heavy metal ions from aqueous solution by APDC impregnated activated carbon. *Talanta*, *67*(1), 59-64.

17. Bhatnagar, A., Hogland, W., Marques, M., & Sillanpää, M. (2013). An overview of the modification methods of activated carbon for its water treatment applications. *Chemical Engineering Journal*, *219*, 499-511.

18. Bazel, Y., Tupys, A., Ostapiuk, Y., Tymoshuk, O., Imrich, J., & Šandrejová, J. (2018). A simple non-extractive green method for the spectrophotometric sequential injection determination of copper (ii) with novel thiazolylazo dyes. *RSC Advances*, *8*(29), 15940-15950.

19. Al-Adilee, K., & Kyhoiesh, H. A. (2017). Preparation and identification of some metal complexes with new heterocyclic azo dye ligand 2-[2−-(1-Hydroxy-4-Chloro phenyl) azo]-imidazole and their spectral and thermal studies. *Journal of Molecular Structure*, *1137*, 160-178.

20. J. Al-Adilee, Khalid & A. Jaber, Sudad. (2018). Synthesis, Characterization and Biological Activities of Some Metal Complexes Derived from Azo Dye Ligand 2-[2'-(5-Methyl thiazolyl)azo]-5-dimethylamino Benzoic Acid. Asian Journal of Chemistry. 30.1537-1545. 10.14233/ajchem.2018.21222.

21. Madu, P. C., & Lajide, L. (2013). Physicochemical characteristics of activated charcoal derived from melon seed husk. *Journal of Chemical and Pharmaceutical Research*, *5*(5), 94-98.

22. Anisuzzaman, S. M., Joseph, C. G., Daud, W. M. A. B. W., Krishnaiah, D., & Yee, H. S. (2015). Preparation and characterization of activated carbon from Typha orientalis leaves. *International Journal of Industrial Chemistry*, *6*(1), 9-21.

23. Pongener, C. H. U. B. A. A. K. U. M., Kibami, D. A. N. I. E. L., Rao, K. S., Goswamee, R. L., & Sinha, D. (2015). Synthesis and characterisation of activated carbon from the biowaste of the plant Manihot esculenta. *Chemical Science Transaction*, *4*(1), 59-68.

24. Habila, M., Yilmaz, E., ALOthman, Z. A., & Soylak, M. (2014). Flame atomic absorption spectrometric determination of Cd, Pb, and Cu in food samples after pre-concentration using 4-(2-thiazolylazo) resorcinol-modified activated carbon. *Journal of Industrial and Engineering Chemistry*, *20*(6), 3989-3993.

25. Aydin, F. A., & Soylak, M. (2010). Separation, preconcentration and inductively coupled plasma-mass spectrometric (ICP-MS) determination of thorium (IV), titanium (IV), iron (III), lead (II) and chromium (III) on 2-nitroso-1-naphthol impregnated MCI GEL CHP20P resin. *Journal of hazardous materials*, *173*(1-3),669-674.

26. Bermejo-Barrera, P., Martinez-Alfonso, N., & Bermejo-Barrera, A. (2001). Separation of gallium and indium from ores matrix by sorption on Amberlite XAD-2 coated with PAN. *Fresenius' journal of analytical chemistry*, *369*(2), 191-194.

27. Maradiya, H. R., & Patel, V. S. (2001). Synthesis and dyeing performance of some novel heterocyclic azo disperse dyes. *Journal of the Brazilian Chemical Society*, *12*(6), 710-714.

28. Fan, X., Zhu, C., & Zhang, G. (1998). Synthesis of 2-[2-(5-methylbenzothiazolyl) azo]-5-dimethylaminobenzoic acid and its application to the spectrophotometric determination of nickel. *Analyst*, *123*(1), 109-112.

29. Mubarak, A. T. (2013). Novel complexes of zirconium and uranium derived from bifunctional azodyes donor ligands containing hydrogen bonds. *Journal of Saudi Chemical Society*, *17*(4), 409-418.

30. Al-Adilee, K. J. (2015). Preparation and Characterization of Some Transition Metal Complexes with NovelAzo-Schiff base Ligand Derived from 2 (E)-(1H-benzo [d] imidazole-2-yly diazenyl)-5-((E)-benzylideneimino) phenol (BIADPI). *RESEARCH JOURNAL OF PHARMACEUTICAL BIOLOGICAL AND CHEMICAL SCIENCES*, *6*(5), 1297-1308.

31. J. Al-Adilee, Khalid & A. Atyha, Saad. (2018). Synthesis, Spectral, Thermal and Biological Studies of Some Metal Complexes Derived from Heterocyclic Mono Azo Dye Ligand 2'[(2'-Hydroxy-4-methyl phenyl)azo]imidazole. Asian Journal of Chemistry. 30. 280-292. 10.14233/ajchem.2018.20889.

32. AL-Adilee, K. J., Abass, A. K., & Taher, A. M. (2016). Synthesis of some transition metal complexes with new heterocyclic thiazolyl azo dye and their uses as sensitizers in photo reactions. *Journal of Molecular Structure*, *1108*, 378-397.

33. Shihad, A. A. A. (2013). *Preparation and Spectrophotometric Study of 2 [2-(5-bromo thiazolyl) azo]-4-methoxy phenol* (Doctoral dissertation, Eastern Mediterranean University (EMU)-Doğu Akdeniz Üniversitesi (DAÜ)).

34. Al-Adilee, K. J., & Shaimaa, A. (2017). Synthesis and spectral Properties studies of novel Hetro Cyclic Mono Azo dyeDerived from Thiazole and Pyridine with Some Transition Complexes. *Oriental journal of chemistry*, *33*(4), 1-14.

35. AL-Adilee, K. J., & Fanfon, D. Y. (2012). Preparation, Spectral Identification and Analytical Studies of Some Transition Metal Complexes with New Thiazolylazo Ligand and Their Biological Activity Study. *Journal of Chemistry and Chemical Engineering*, *6*(11), 1016.

36. AL-Adilee, K. J., Abass, A. K., & Taher, A. M. (2016). Synthesis of some transition metal complexes with new heterocyclic thiazolyl azo dye and their

uses as sensitizers in photo reactions. *Journal of Molecular Structure*, *1108*, 378-397.

37. Prahas, D., Kartika, Y., Indraswati, N., & Ismadji, S. (2008). Activated carbon from jackfruit peel waste by H3PO4 chemical activation: pore structure and surface chemistry characterization. *Chemical Engineering Journal*, *140*(1-3), 32-42.

38. Anisuzzaman, S. M., Joseph, C. G., Taufiq-Yap, Y. H., Krishnaiah, D., & Tay, V.V. (2015). Modification of commercial activated carbon for the removal of 2, 4-dichlorophenol from simulated wastewater. *Journal of King Saud University-Science*, *27*(4), 318-330.

39. Sahira, J., Mandira, A., Prasad, P. B., & Ram, P. R. (2013). Effects of activating agents on the activated carbons prepared from lapsi seed stone. *Res J Chem Sci*, *3*(5), 19.

40. Abazari, R., Mahjoub, A. R., & Sanati, S. (2014). A facile and efficient preparation of anatase titania nanoparticles in micelle nanoreactors: morphology, structure, and their high photocatalytic activity under UV light illumination. *RSC Advances*, *4*(99), 56406-56414.

41. Al-Adilee, K. J. (2018). Synthesis, Spectral and Biological Studies of Metal Complexes with Heterocyclic Ligand Derived from Thaizolylazo Dye. *Journal of Global Pharma Technology*.

42. Bai, S., Hu, J., Li, D., Luo, R., Chen, A., & Liu, C. C. (2011). Quantum-sized ZnO nanoparticles: synthesis, characterization and sensing properties for NO2. *Journal of Materials Chemistry*, *21*(33), 12288-12294.

43. Gottipati, R. (2012). *Preparation and characterization of microporous activated carbon from biomass and its application in the removal of chromium (VI) from aqueous phase* (Doctoral dissertation).

44. Liou, T. H. (2010). Development of mesoporous structure and high adsorption capacity of biomass-based activated carbon by phosphoric acid and zinc chloride activation. *Chemical Engineering Journal*, *158*(2), 129-142.

45. Sivachidambaram, M., Vijaya, J. J., Kennedy, L. J., Jothiramalingam, R., Al-Lohedan, H. A., Munusamy, M. A., ... & Merlin, J. P. (2017). Preparation and characterization of activated carbon derived from the Borassus flabellifer flower as an electrode material for supercapacitor applications. *New Journal of Chemistry*, *41*(10), 3939-3949.

46. Vellaichamy, S., & Palanivelu, K. (2011). Preconcentration and separation of copper, nickel and zinc in aqueous samples by flame atomic absorption spectrometry after column solid-phase extraction onto MWCNTs impregnated with D2EHPA-TOPO mixture. *Journal of hazardous materials*, *185*(2-3), 1131-1139.

47. Asci, B., Alpdogan, G., & Sungur, S. (2006). Preconcentration of some trace metal ions from drinking and tap water samples by sorption on Amberlite XAD-4 after complexation with di-2-pyridyl ketone thiosemicarbazone. *Analytical letters*, *39*(4-6), 997-1007.

48. Cesur, H. (2003). Determination of manganese, copper, cadmium and lead by FAAS after solid-phase extraction of their phenylpiperazine dithiocarbamate complexes on activated carbon. *Turkish Journal of Chemistry*, *27*(3), 307-314.